

Accurate quantitative phase imaging through telecentric digital holographic microscopy

Ana Doblas, Emilio Sánchez-Ortiga, Manuel Martínez-Corral, Genaro Saavedra

Department of Optics, University of Valencia, E-46100 Burjassot, Spain.
a.isabel.doblas@uv.es, Emilio.Sanchez@uv.es, Manuel.Martinez@uv.es, Genaro.Saavedra@uv.es

Jorge Garcia-Sucerquia

Universidad Nacional de Colombia Sede Medellin, School of Physics, A.A: 3840, Medellin 050034, Colombia
jgarcia@unal.edu.co

ABSTRACT

The use of non-telecentric imaging systems in quantitative phase digital holographic microscopy introduces strong inaccuracies. We show that even negligible errors in the radius and center of curvature of the remaining quadratic phase factor introduce big errors in the numerical phase measurements. The errors depend on the position of the object in the field-of-view. However, when a telecentric imaging system is utilized for the recording of the holograms, the hybrid imaging method shows shift-invariant behavior, and therefore accurate quantitative phase imaging can be performed.

Key words: Digital Holographic Microscopy, Quantitative Phase Imaging

Digital holographic microscopy (DHM) allows to retrieve the quantitative phase of microscopic samples through the recovering of the complex amplitude distribution of the field diffracted by them [1]-[4]. This information can be used for both numerical refocusing to different planes and performing quantitative measurements inasmuch as the phase of the field is accessible. The differences in the measured phase are directly related with changes of index of refraction within the sample. For homogeneous samples, that is, for samples with a constant index of refraction n , the quantitative phase gives information of their tridimensional shape. This characteristic makes DHM a unique technique for the inspection and characterization of *in vivo* label-free samples [5]-[7]. A digital hologram is the recording by means of a digital camera of the interference between the wavefield diffracted by an object (with amplitude transmittance labeled as $o(\mathbf{x}, z)$) and a beam without amplitude information $R(\mathbf{x}, z)$, named the reference beam. In general the reference beam can take any curvature but, for simplicity, we consider it a plane wave. This implies that the reference beam can mathematically expressed as

$$R(\mathbf{x}, z) \propto \exp(i \mathbf{k} \cdot \mathbf{x}), \quad (1)$$

being $\mathbf{x}=(x,y)$ the transverse coordinates and \mathbf{k} the wave-vector, which contains the information of the wavelength λ and the angle of the reference beam with respect to the optical axis. In the case of off-axis DHM the reconstruction process only requires one-shot. The intensity distribution of the field generated by the interference between the reference and the object beams in the plane where the camera is placed is given by

$$I_H(\mathbf{x}) = |o'(\mathbf{x}, d)|^2 + |R(\mathbf{x}, d)|^2 + R^*(\mathbf{x}, d)o'(\mathbf{x}, d) + R(\mathbf{x}, d)o'^*(\mathbf{x}, d), \quad (2)$$

where

$$o'(\mathbf{x}, d) = o'(\mathbf{x}) \otimes_2 \exp\left(\frac{ik}{2d}|\mathbf{x}|^2\right), \quad (3)$$

is the propagation to the recording distance d of the image complex amplitude $o'(\mathbf{x})$ provided by the MO, and

$k = 2\pi/\lambda$ is the wavenumber. The shape of $o'(\mathbf{x})$ depends on the imaging system employed for recording the digital hologram. Typically, the MO used for performing the imaging process is finite-conjugated. When using this kind of MO the output field in the image space is given by a spherical wave that carries the information of the sample, both in amplitude and phase. The remaining curvature phase factor introduced by the MO affects the imaging conditions of the DHM. It has been shown that numerical methods can compensate the phase factor in the last step of the processing, that is, after properly filtering the Fourier space of the digital hologram and compensating the reference beam [8]-[10]. The process for removing the phase curvature includes an unwrapping of the phase and a polynomial fitting of the spherical phase factor. By doing this, the parameters of the polynomial fitting should match not only the curvature of the factor but also its center of curvature. Slight errors in this determination produce undesired effects in the final quantitative phase image [11]. Other proposal for removing the factor suggests the capturing of a digital hologram without object. The resulting phase map of this hologram is subtracted to the one including the object. This process removes the spherical phase produced by the MO [12], but requires two shot and the acquisition of a new digital hologram without object when the illumination conditions change. It is noticeable that the difficulties attaining the spherical phase factor can be eliminated by means of the use of an afocal-telecentric arrangement [13]. This optical composite includes an infinite-conjugated MO and a tube-lens (TL) in afocal (the back focal plane of the MO and the front focal plane of the TL are in the sample plane) and telecentric (the entrance pupil is in the front focal plane of the TL) configuration. In the following we recapitulate the benefits of acquiring digital holograms with an optical compensation of the phase factor.

With the aim of comparing the system when the image complex amplitude is affected by a spherical phase factor with the afocal-telecentric one, we have designed the following scheme: the microscope is composed by a tube-lens of focal length f_{TL} with a variable distance l to an infinite-corrected MO. Then, the curvature of the output field will depend on the parameter l . It can be shown that the complex amplitude in the image plane of the system is given by

$$o'(\mathbf{x}) = \exp\left[\frac{ik}{2C}|\mathbf{x}|^2\right] \left\{ \frac{1}{M} o\left(\frac{\mathbf{x}}{M}\right) \otimes_2 \tilde{p}\left(\frac{\mathbf{x}}{\lambda f_{TL}}\right) \right\}, \quad (4)$$

where M is the lateral magnification of the microscope, $C = f_{TL}^2/(f_{TL} - l)$ is the curvature radius and $p(\mathbf{x})$ is the pupil function of the system. Then a variation of the distance l leads to a change in the curvature of the image wavefront. Then, for an afocal-telecentric system $l=f_{TL}$ so the curvature radius tends to infinite. In that case, as expected, the spherical phase factor vanishes.

In order to extract the information of interest from the digital hologram, that is, the image complex amplitude distribution $o'(\mathbf{x}, d)$, the Fourier transform of the Eq.(2) is performed:

$$\tilde{I}_H(\mathbf{u}) = DC(\mathbf{u}, d) + \tilde{o}'(\mathbf{u}, d) \otimes_2 \delta(\mathbf{u} - \mathbf{k}) + \tilde{o}'^*(\mathbf{u}, d) \otimes_2 \delta(\mathbf{u} + \mathbf{k}). \quad (5)$$

In this space we have 3 terms: the +1 and -1 orders containing the same but complex conjugated information and the DC order which is the Fourier transform of the intensity terms. The +1 and -1 orders are symmetrically displaced over the center of coordinates to a frequency \mathbf{k} . Under the proper conditions [14], the three terms can be isolated from each other permitting to extract only the complex amplitude distribution of the object beam. In order to compensate the reference beam angle a shifting of the filtered +1 order is performed. The remaining Fourier space can be written as

$$\tilde{I}_H^{+1}(\mathbf{u} - \mathbf{k}) = \tilde{I}_H(\mathbf{u} - \mathbf{k}) \cdot F(\mathbf{u}) \quad (6)$$

being $F(\mathbf{u})$ a generic binary filter. For simplicity, we consider that the recording distance is zero, that is, we assume that

the digital hologram is captured in the image plane of the microscope. If the parameters of the system meet the conditions attaining the number (N_x, N_y) and size of the camera pixels (Δp), the value of \mathbf{k} , and the numerical aperture (NA) and the M value of the microscope for recording a diffraction limited hologram and avoiding the overlapping of Fourier orders, then $F(\mathbf{u})$ can be applied in such a way that

$$\tilde{I}_H^{+1}(\mathbf{u} - \mathbf{k}) = \tilde{o}'(\mathbf{k}) = \exp\left[-i\pi\lambda C|\mathbf{u}|^2\right] \otimes_2 \left\{ \tilde{o}(M\mathbf{u}) p(\lambda f_{TL} \mathbf{u}) \right\}. \quad (7)$$

In Eq.(7) we identify a first undesired effect caused by the use of an optical configuration that induces a curvature into the object beam. The image spectrum is convolved by a spherical phase factor. This convolution involves an expansion of the image spectrum directly proportional to the curvature induced by the microscope. In Fig.1 we can see a numerical simulation of the expansion of the +1 order for a diffraction limited digital hologram of an USAF 1951 test target ($N_x=N_y=1024$, $\Delta p=6.9\mu\text{m}$). The image in the left corresponds to an afocal-telecentric system, whereas in the middle and the right ones the curvatures were equal to 400mm and 300 mm, respectively.

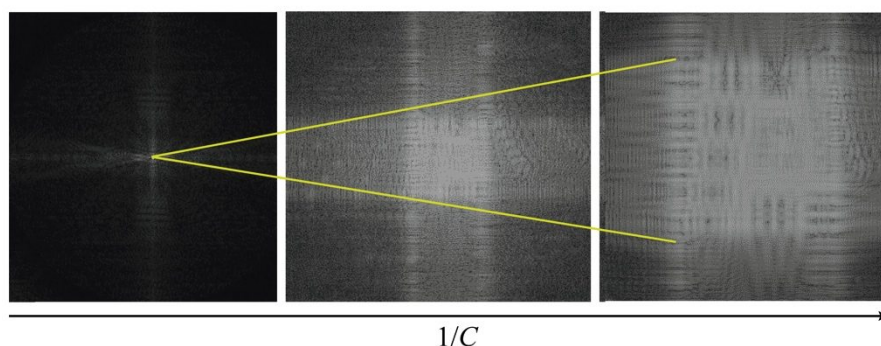


Figure 1 Shape of the +1 order of a diffraction limited digital hologram of a USAF 1951 test target as function of the curvature. The cases are: (Left) $1/C$ is zero, that is, when the system is afocal-telecentric, and $1/C$ taken the values 400mm (Center) and 400mm(Right).

As it can be seen, the filtering conditions when using a finite-conjugated MO (or an optical system producing a spherical distortion in the object arm with any curvature) are more restrictive and less intuitive. The effective curvature and then the spreading of the +1 and -1 orders depends on the size of the sensor. It is found that the bandwidth occupied by the +1 order is given by a rectangle of sides [14]

$$L_x = \frac{N_x \Delta p}{\lambda C}, \quad L_y = \frac{N_y \Delta p}{\lambda C}, \quad (7)$$

Taking into account that the size of the DC term is twice of the pupil radius (as it is given by the autocorrelation of the image complex amplitude distribution) and it does not depend on the curvature of the object wavefront, the usable space-bandwidth depends not only on the value of $1/C$, but also on the size of the digital hologram. On the contrary, the size of the terms in the afocal-telecentric case is well established by the pixel size. In this case a proper spatial filtering can be always done if the pupil function radius accomplish the following condition

$$\rho_{TM} \leq \frac{1}{\sqrt{2}(\sqrt{2}+3)\Delta p}. \quad (8)$$

For a given sensor we can find a value of $1/C$ that implies a practical loss of the digital hologram bandwidth in comparison with the bandwidth when $C \rightarrow \infty$. This effect is illustrated in Fig.2: the Fourier space of our numerical simulation for an afocal-telecentric system (panel a) and for a system with a spherical phase factor driven by a curvature of 266mm (panel b) are represented. In both cases we can find a value of the pupil radius, ρ_{TM} and ρ_{NTM} respectively, which permits to isolate the +1, -1 and DC orders from each other. However, the size of the pupil should be decreased for avoiding the overlapping between terms due to the expansion of the +1 and -1 orders when the spherical phase factor is affecting the system. Ultimately, this means that the system has lower resolution than in the case of an afocal-telecentric configuration if the same imaging conditions are considered.

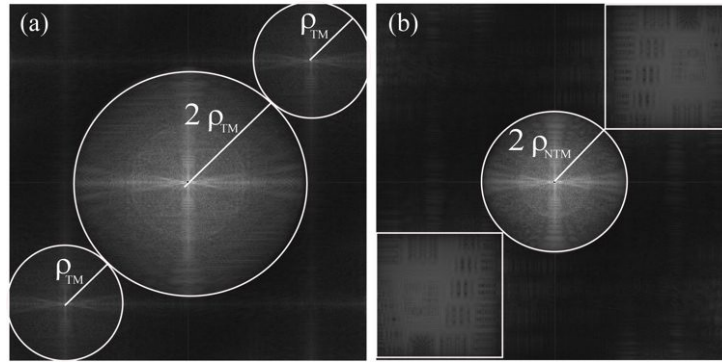


Figure 2 Simulation of the Fourier space of a digital hologram of a USAF 1951 test target when optimizing the space bandwidth for (a) afocal-telecentric system, and (b) spherical distortion with a value of $C=266\text{mm}$.

After performing the proper filtering of the digital hologram Fourier space, we perform the inverse Fourier transform

$$o'_{rec}(\mathbf{x}) = \mathfrak{F}\left(\tilde{I}_H^{+1}(\mathbf{u}-\mathbf{k})\right). \quad (9)$$

The quantitative phase of the image complex amplitude distribution can be obtained by

$$\phi(\mathbf{x}) = \tan^{-1}\left(\frac{\text{Im}(o'_{rec}(\mathbf{x}))}{\text{Re}(o'_{rec}(\mathbf{x}))}\right). \quad (10)$$

It is straightforward to see that the quantitative phase image is given by

$$\phi(\mathbf{x}) = \text{mod}\left[\frac{ik}{2C}|\mathbf{x}|^2 + \phi_o(\mathbf{x}), 2\pi\right], \quad (11)$$

where $\phi_o(\mathbf{x})$ is the quantitative phase of the image. As the retrieved phase is defined in modulus 2π , an unwrapping algorithm should be applied. However, in most practical cases the samples are thin and there is no wrapping of the quantitative phase owing to the term $\phi_o(\mathbf{x})$, but the unwrapping is needed for compensating the undesired phase factor. For removing the spherical phase a polynomial fitting of the area of $\phi(\mathbf{x})$ free of sample information is usually done. In practice, the center of curvature does not match the central pixel of the camera. Consequently, the fitting should provide not only the value of C , but also the coordinates in which the center of curvature is located. For the case of an

afocal-telecentric system ($C \rightarrow \infty$) the quantitative phase image is directly obtained.

It follows that the use of the afocal-telecentric arrangement reduces the number of calculations needed for the representation of the quantitative phase of the sample. In the same way, the possible sources of error are less: if the spherical phase factor is present, the system has 4 degrees of freedom (\mathbf{k} , C and the coordinates of the center of curvature) whereas for the afocal-telecentric system there is only one degree of freedom, the reference beam angle. For showing the benefits of using the afocal-telecentric system instead of any other system producing a spherical wavefront distortion, we used the experimental setup illustrated in Fig. 3. The system is a DHM based on the Mach-Zehnder interferometer scheme: two beams splitter (BS1, BS2) and two mirrors (M1, M2) are used for firstly splitting a collimated beam ($\lambda=632.8\text{nm}$) into the object and reference beams and, secondly, for producing the interference of both beams into a CCD camera (1248×1024 pixels with $\Delta p=6.9\mu\text{m}$). The reference angle is ruled by the angle of BS2. As stated above, we used a system that permits a variable value of the curvature induced by MO consisting of an infinite-corrected MO and a TL of $f_{\text{TL}}=200$ mm with their foci separated a distance l .

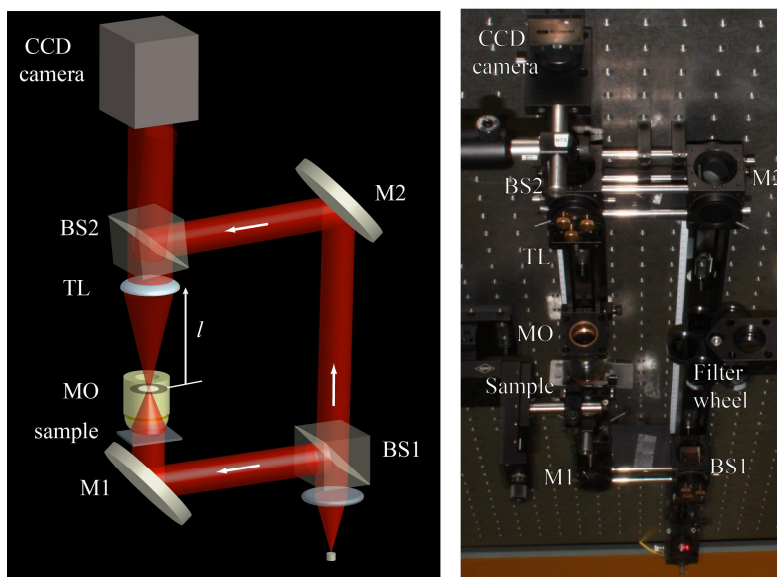


Figure 3 Off-axis DHM system with variable curvature of the wavefront: (left) scheme and (right) experimental setup.

As a first example we acquired two digital holograms of a slice of the head of a drosophila melanogaster by using a MO $10\times$ of $\text{NA}=0.45$. These are captured for a system with $l=180\text{mm}$ and for an afocal-telecentric system. The phase-map directly obtained with the system when the spherical phase factor is present is shown in Fig. 4(a). After the application of an unwrapping algorithm (Goldstein algorithm) a polynomial fitting of the phase factor in zones without sample information was done for compensating the spherical phase factor. The resulting phase-map after the spherical phase removal is shown in Fig. 4(b). As it can be seen, in that case numerical errors were introduced in the final quantitative phase image. In the case of an afocal-telecentric system, the quantitative phase obtained is shown in Fig. 5. In that case, the obtained phase-map is free of noise and it represents directly the function $\phi_o(\mathbf{x})$.

Thus the use of an afocal telecentric system gives more stability to the system and it allows a quicker reconstruction as the number of operations is reduced. Strictly, if we consider the capturing of the digital hologram of a thin sample in the image plane of the imaging system, the reconstruction process only requires two Fast-Fourier transforms, the spatial filtering and the reference beam angle matching. For homogenous samples, the quantitative phase can be

easily related with the variation in depth, Δh , through the optical path length (OPL) which drives to the formula

$$\Delta h(\mathbf{x}) = \frac{\lambda \phi(\mathbf{x})}{2\pi \Delta n}, \quad (11)$$

being Δn the difference between the index of refraction of the sample and the one of the medium in which the sample is immersed. An example of the 3D representation of the depth measurement obtained from the afocal-telecentric DHM (50x, NA=0.5) for a label-free red blood cell sample is shown in Fig. 6.

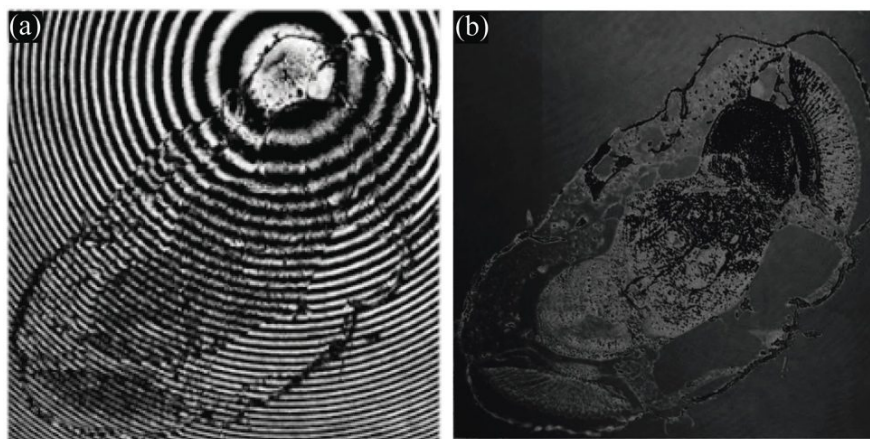


Figure 4 Results obtained with DHM for drosophila melanogaster head slice when the system is affected by the phase factor introduced by the MO (10x, NA=0.45) (a) Wrapped phase map. (b) Reconstructed wavefront after applying the numerical compensation of the spherical phase.

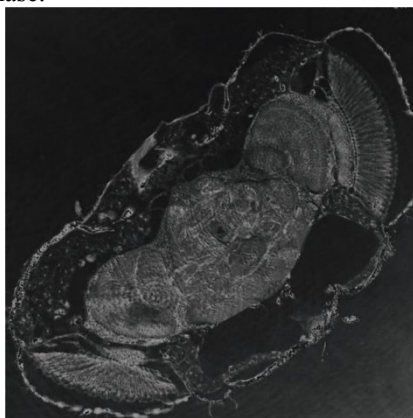


Figure 5 Quantitative phase image directly obtained from the digital hologram of a drosophila melanogaster head for the afocal-telecentric DHM.

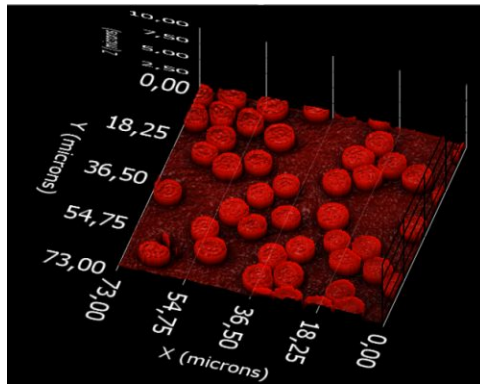


Figure 6 3D representation of the quantitative measurement of red blood cells by using the afocal-telecentric DHM.

As conclusion, the use of afocal-telecentric microscopes eases the reconstruction process as it reduces the number of calculations, guarantees that the system is limited by diffraction as the filtering process is made in the “proper” Fourier space, and also diminishes the degrees of freedom for obtaining quantitative phase measurements what avoids the sources of possible errors. The latter is of great importance as DHM is stated to have a high precision in the determination of changes in the OPL within the sample.

ACKNOWLEDGEMENTS

Financial support by the Ministerio de Economía y Competitividad, Spain (Grant DPI2012-32994) and the Generalitat-Valenciana (Grant PROMETEO2009-077) is gratefully acknowledged. A. Doblas greets funding from the University of Valencia through the predoctoral fellowship program “Atracció de Talent”. J. Garcia-Sucerquia gratefully acknowledges the financial support from the Universidad de Valencia, Spain, under the Program “Estancias Temporales para Investigadores Invitados”, Colciencias grant number 110205024 and UNAL grants numbers 110201003 and 110201004.

REFERENCES

- [1] U. Jüptner, and W. Schnars, “Direct recording of holograms by a CCD target and numerical reconstruction,” *Appl. Opt.* **33**, 179-181 (1994).
- [2] E. Cucho, F. Bevilacqua, and C. Depeursinge, “Digital holography for quantitative phase-contrast imaging,” *Opt. Lett.* **24**, 291-293 (1999).
- [3] M. K. Kim, “Principles and techniques of digital holographic microscopy,” *SPIE Reviews* **1**, 018005 (2010).
- [4] E. Cucho, P. Marquet, and C. Depeursinge, “Simultaneous amplitude-contrast and quantitative phase-contrast microscopy by numerical reconstruction of Fresnel off-axis holograms,” *Appl. Opt.* **38**, 6994-7001 (1999).
- [5] N. Pavillon, J. Kühn, C. Moratal, P. Jourdain, C. Depeursinge, P. J. Magistretti, and P. Marquet, “Early cell death detection with digital holographic microscopy,” *PLoS ONE* **7**, 30912 (2012)
- [6] B. Kemper, A. Bauwens, A. Vollmer, S. Ketelhut, P. Langehanenberg, J. Mütihng, H. Karch, and G. von Bally, “Label-free quantitative cell division monitoring of endothelial cells by digital holographic microscopy,” *J. Biomed. Opt.* **15**, 036009 (2010)
- [7] C. J. Mann, L. Yu, and M. K. Kim, “Movies of cellular and sub-cellular motion by digital holographic microscopy,” *Biomed. Eng. Online* **5**, 1-10 (2006).
- [8] T. Colomb, J. Kühn, F. Charière, and C. Depeursinge, “Total aberrations compensation in digital holographic microscopy with a reference conjugated hologram,” *Opt. Express* **14**, 4300-4306 (2006).

- [9] F. Montfort, F. Charrière, T. Colomb, E. Cuche, P. Marquet, and C. Depeursinge, "Purely numerical compensation for microscope objective phase curvature in digital holographic microscopy: influence of digital phase mask position," *J. Opt. Soc. Am. A* **23**, 2944–2953 (2006).
- [10] K. W. Seo, Y. S. Choi, E. S. Seo, and S. J. Lee, "Aberration compensation for objective phase curvature in phase holographic microscopy," *Opt. Lett.* **37**, 4976–4978 (2012).
- [11] A. Doblas, E. Sánchez-Ortiga, M. Martínez-Corral, G. Saavedra, P. Andrés, and J. Garcia-Sucerquia, "Shift-variant digital holographic microscopy: inaccuracies in quantitative phase imaging," *Opt. Lett.* **38**, 1352–1354 (2013).
- [12] P. Ferraro, S. De Nicola, A. Finizio, G. Coppola, S. Grilli, C. Magro, and G. Pierattini, "Compensation of the Inherent Wave Front Curvature in Digital Holographic Coherent Microscopy for Quantitative Phase-Contrast Imaging," *Appl. Opt.* **42**, 1938–1946 (2003).
- [13] E. Sánchez-Ortiga, P. Ferraro, M. Martínez-Corral, G. Saavedra, and A. Doblas. "Digital holographic microscopy with pure-optical phase compensation," *J. Opt. Soc. Am. A* **28**, 1410–1417 (2011).
- [14] E. Sánchez-Ortiga, A. Doblas, G. Saavedra, M. Martínez-Corral, and J. Garcia-Sucerquia, "Off-axis Digital Holographic Microscopy: practical design parameters for operating at diffraction limit," *Appl. Opt.* **53**, 2058–2066 (2014).